

# SMA-STN: Segmented Movement-Attending Spatiotemporal Network for Micro-Expression Recognition

Jiateng Liu<sup>1</sup>, Wenming Zheng<sup>1</sup>, Yuan Zong<sup>1</sup>

<sup>1</sup> School of Biological Science and Medical Engineering, Southeast University, Nanjing, China  
jiateng\_liu@seu.edu.cn, wenming\_zheng@seu.edu.cn, xhzongyuan@seu.edu.cn

## Abstract

Correctly perceiving micro-expression is difficult since micro-expression is an involuntary, repressed, and subtle facial expression, and efficiently revealing the subtle movement changes and capturing the significant segments in a micro-expression sequence is the key to micro-expression recognition (MER). To handle the crucial issue, in this paper, we firstly propose a dynamic segmented sparse imaging module (DSSI) to compute dynamic images as local-global spatiotemporal descriptors under a unique sampling protocol, which reveals the subtle movement changes visually in an efficient way. Secondly, a segmented movement-attending spatiotemporal network (SMA-STN) is proposed to further unveil imperceptible small movement changes, which utilizes a spatiotemporal movement-attending module (STMA) to capture long-distance spatial relation for facial expression and weigh temporal segments. Besides, a deviation enhancement loss (DE-Loss) is embedded in the SMA-STN to enhance the robustness of SMA-STN to subtle movement changes in feature level. Extensive experiments on three widely used benchmarks, i.e., CASME II, SAMM, and SHIC, show that the proposed SMA-STN achieves better MER performance than other state-of-the-art methods, which proves that the proposed method is effective to handle the challenging MER problem.

## Introduction

Micro-expression is a kind of unique facial expression usually occurring when people try to hide their genuine underlying emotions, which is subtle, involuntary, and has a short duration of only  $\frac{1}{25}$ s to  $\frac{1}{5}$ s (Ekman and Friesen 1969). Haggard et al. (Haggard and Isaacs 1966) first discovered the micro-expression during the research of ego mechanisms in psychotherapy. And then, Ekman et al. (Ekman and Friesen 1969) rediscovered this type of facial expression when looking at a video of psychopath and named it micro-expression officially. Unlike regular facial expressions, micro-expression is imperceptible and can reveal humans' real emotions what they want to conceal. Thus, automatically recognizing the micro-expression has many practical applications, such as criminal investigation, lie detection, and clinical diagnosis (Frank et al. 2009)(O'Sullivan et al. 2009)(Frank, Maccario, and Govindaraju 2009).

Copyright © 2021, Association for the Advancement of Artificial Intelligence (www.aaai.org). All rights reserved.

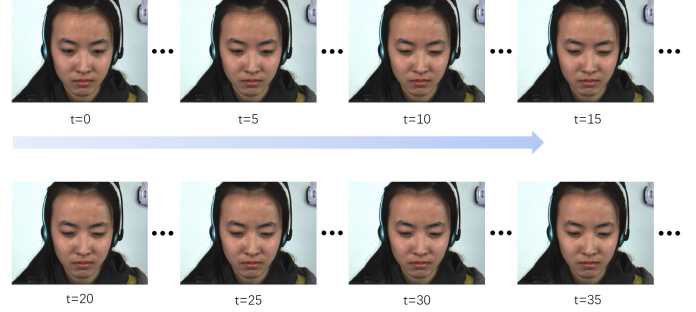


Figure 1: A sample sequence of micro-expression, where  $t$  stands for time order. Since the subtle and involuntary changes of micro-expression, a number of frame samples are similar to each other, which are redundant for recognition.

However, due to the characteristics of short duration and low intensity of micro-expression, realizing the automatic micro-expression recognition is still a very challenging task than conventional facial expression recognition problems, and even the person with professional training could get only 47% accuracy in MER. (Frank et al. 2009) As shown in Figure 1, since the movement changes in a micro-expression sequence are incredibly subtle, many adjacent micro-expression data frames are similar to each other, and it is evident that capturing the segments which contains more subtle movement information can improve MER a lot. According to (Wang et al. 2016), it is unnecessary to sample frames densely in a video sequence due to the information redundancy of adjacent frames. Hence, it is necessary to efficiently sample data to accurately extract spatiotemporal information of micro-expressions and suppress segments which contains less useful information for MER, and the traditional feature extraction methods for regular facial expressions are obviously not suitable to the micro-expressions. Furthermore, it is tough to discern the movement changes of micro-expressions for the the traditional spatiotemporal approaches due to the short duration. The aforementioned issues are usually ignored by the traditional handcraft methods or CNN-based approaches for MER.

To handle the crucial problems of MER, we first propose a novel dynamic representation extraction approach dubbed

dynamic segmented sparse imaging module (DSSI) in this paper. Given a micro-expression sequence, DSSI firstly samples four sets of micro-expression data images from different segments of a sequence under a unique protocol. Each set contains three micro-expression images to compute a micro-expression dynamic images based on dynamic imaging method (Bilen et al. 2017)(Bilen et al. 2016). DSSI can not only reveal subtle movement changes through capturing the micro-level spatiotemporal features of different segments in a micro-expression sequence, but also avoid the interference of useless data frames on MER. Secondly, we propose a segmented movement-attending spatiotemporal network (SMA-STN) to weigh different ME dynamic images and further unveil the subtle movement changes. The main components of SMA-STN include a CNN backbone and a spatiotemporal movement-attending module (STMA). The CNN backbone extracts spatiotemporal features from the computed dynamic images. And then, the spatiotemporal movement-attending module learns attention weights for different segments to capture both the global context information of a micro-expression sequence and the long-range dependencies of facial expression simultaneously by utilizing two types of self-attention mechanisms, including a global self-attention module and a non-local self-attention block. Subsequently, the processed dynamic features are aggregated to a global representation with calculated attention weights for the final classification. Furthermore, we also propose a deviation enhancement loss (DE-Loss) function embedded in the SMA-STN to further magnify the discrepancies of dynamic images generated from different segments of a micro-expression sequence, so that we can further improve the robustness of SMA-STN for subtle movement changes. Extensive experiments on three widely used micro-expression benchmarks show that the proposed model has strong robustness to subtle movement changes in a micro-expression sequence and can capture the representative spatial-temporal micro-expression features samples efficiently.

In a word, our contributions can be summarized as follows:

- 1) We propose a novel dynamic representation extraction approach termed dynamic segmented sparse imaging module (DSSI) to capture the subtle movement changes while reducing the redundant data for MER.
- 2) We propose a novel segmented movement-attending spatiotemporal network (SMA-STN) combined with a CNN backbone and a novel spatiotemporal movement-attending module (STMA) to extract representative features. SMA-STN can handle the crucial issue of capturing long-distance spatial relations of facial expression and weighting for different micro-expression sequence segments simultaneously.
- 3) A deviation enhancement loss (DE-Loss) function embedded in the SMA-STN is also proposed to magnify the micro-level movement discrepancies between different segments of a ME sequence further.

## Related Work

### Micro-Expression Recognition

Previous researches about MER usually focus on extracting robust spatiotemporal features. In (Pfister et al. 2011), Pfister et al. firstly investigated the micro-expression recognition problem by using local binary pattern from three orthogonal planes (LBP-TOP) to describe the spatiotemporal characteristics of micro-expression video clips. Through their experimental results, the LBP-TOP feature is proved to be effective for the MER issue. Besides, they also utilized a temporal interpolation model (TIM) to normalize the number of micro-expression frames into a fixed size. In (Polikovsky, Kameda, and Ohta 2009), Polikovsky et al. proposed a 3D-gradients orientation histogram-based feature descriptor to investigate the MER problem. In addition, Wang et al. (Wang et al. 2014) used robust principal component analysis (RPCA) to extract the background information, and then both of LBP-TOP and Local Spatiotemporal Directional Features (LSDF) are used for MER. In (Liu, Li, and Lai 2018), Liu et al. proposed a sparse main directional mean optical-flow (Sparse MDMO) feature as a novel distance metric to learn a practical dictionary from micro-expression data samples, which can be computed easily.

With the development of deep learning recently, many researchers put forward a series of deep convolutional neural networks (CNNs) based methods to conduct MER, which achieved impressive results. For example, Verma et al. (Verma et al. 2019) proposed a Lateral Accretive Hybrid network (LearNet) to spot the involuntary changes in a micro-expression sequence and classify them. In (Xia et al. 2019), Xia et al. first considered the spatiotemporal deformations of micro-expression samples by utilizing deep model named spatiotemporal recurrent convolutional networks (STRCN) with two types of extension. Furthermore, Song et al. (Song et al. 2019) proposed a three-stream convolution network (TSCNN) combined with a dynamic-temporal stream, a static-spatial stream and a local-spatial stream to aggregate temporal information and local region cues of micro-expressions for recognizing. Nevertheless, the inability to capture subtle movement changes and capture the significant segments of a micro-expression sequence in a efficient way is often neglected by these methods.

### Attention Mechanisms In Deep Learning

The attention mechanism is widely used in various fields including computer vision, natural language processing and so on (Vaswani et al. 2017). With the development of deep learning in recent years, numerous works have applied attention mechanism to deep neural networks, which achieved excellent performance (Meng et al. 2019)(Yang et al. 2017)(Wang et al. 2019). In (Yang et al. 2017), Yang et al. proposed a Neural Aggregation Network (NAN) for video face recognition. They utilized attention to aggregate facial features of a person into a compact and fixed-dimension feature representation for recognition based on a deep convolutional neural network. Similarly, Wang et al. (Wang et al. 2019) proposed a region attention network (RAN) to handle the pose and occlusion variant facial ex-

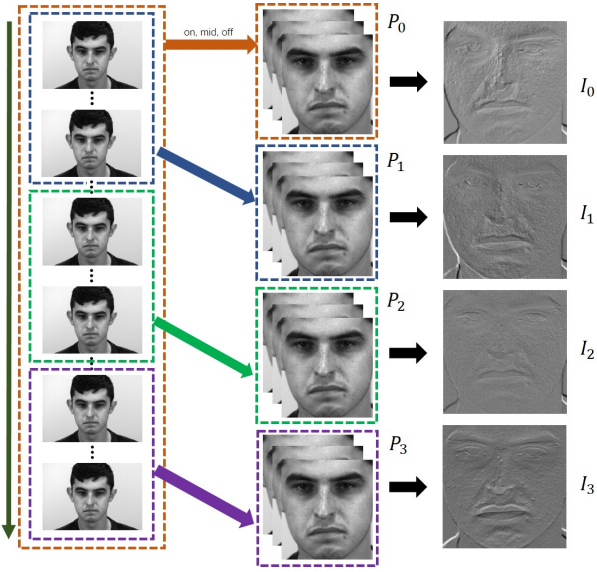


Figure 2: The illustration of DSSI. Given a sequence of micro-expressions, we first do the pre-processing for micro-expression samples. Subsequently, DSSI divides the sequence into three segments evenly and sparsely samples three frames from each segment to generate three snippets  $\{P_1, P_2, P_3\}$ . Especially, a snippet  $P_0$  consists of the onset, middle and offset frames of the sequence are also obtained. Finally, four dynamic images  $\{I_0, I_1, I_2, I_3\}$  are computed by utilizing the obtained snippets in total.

pression recognition problem. They aggregated and embedded a varied number of region features produced by a self-attention module and a relation-attention module into a compact fixed-dimension feature representation before classification. In (Wang et al. 2018), Wang et al. proposed several non-local attention frameworks to capture the long-range interactions among distant pixels in both spatial and temporal fields. The core idea of the non-local operation is also a self-attention mechanism and it achieved promising performance in many tasks, including video classification, object detection and pose estimation. Inspired by the various self-attention mechanisms, we design a novel spatiotemporal movement-attending module to capture the long-distance spatial relation for facial regions and learn importance weights for different segments of a micro-expression sequence at the same time.

## Proposed Methods

This section describes the whole framework in detail. As shown in Figure 2, given a sequence of micro-expression samples, DSSI computes four dynamic images as local-global spatiotemporal descriptors under a special sampling protocol. The computed micro-expression dynamic images are then fed into the CNN backbone for feature extraction as shown in Figure 3. Subsequently, the spatial non-local self-attention module processes the dynamic features to capture the long-range dependencies with a special non-local attention block. The global self-attention module weighs

each segment by a fully-connected layer and the sigmoid function to enhance the most significant dynamic image. Besides, a deviation enhancement loss is further proposed to measure the micro-level discrepancies between different segments and magnify them. The final global representation is aggregated with the segment feature for classification.

## Dynamic Segmented Sparse Imaging

According to (Wang et al. 2016), it would be efficient to sample frames with a sparse and global temporal strategy to capture the long-range video representation since consecutive frames are highly redundant. Besides, the short duration of micro-expressions make a consequence that not all the micro-expression frames are useful to the micro-expression recognition, and the traditional feature extraction approaches for MER can not reflect overall information objectively. Motivated by the dynamic imaging technology (Verma et al. 2019)(Bilen et al. 2017)(Bilen et al. 2016) and sparse sampling mechanism (Wang et al. 2016), we propose a novel dynamic representation extraction approach, namely dynamic segment sparse imaging (DSSI) module, to compute dynamic images in different segments as local-global spatiotemporal descriptors so that we can capture the subtle movement changes of a micro-expression sequence while reducing redundant micro-expression frames.

**Sparse Sampling.** The illustration of dynamic segmented sparse sampling is shown in Figure 2. Given a sequence of micro-expression sample  $V$ , we first divide it into 3 segments  $\{S_1, S_2, S_3\}$  of equal duration without overlap after pre-process. For each segment, we then divide it into 3 equal sub-segment again, i.e.  $S_i = \{s_i^1, s_i^2, s_i^3\}$ . Finally, DSSI randomly samples a micro-expression instance snippet  $P_i = \{P_i^0, P_i^1, P_i^2\}$  from each sub-segment in each segment. To capture global spatiotemporal information of a micro-expression sequence, a snippet including the onset, middle and offset frames of the sequence is also obtained as a comparison, i.e.,  $P_0 = \{P_0^{on}, P_0^{mid}, P_0^{off}\}$ .

**Dynamic Imaging.** The core idea of dynamic imaging method is to represent a video by a single RGB image based on rank pooling (Bilen et al. 2017)(Bilen et al. 2016). Supposing that a micro-expression sequence is represented as a ranking function by its frames  $\{R_1, R_2, \dots, R_t\}$ . Let  $V_i = \frac{1}{i} \sum_{t=1}^i \psi(R_t)$  be time average of these features up to time  $t$ , where  $\psi_t$  is the representation vector extracted from each individual frame  $R_t$  of the video sequence. Then the ranking function calculates a score to associate each time  $t$  by  $S(t|d) = \langle d, V_t \rangle$ , where  $d \in \mathbb{R}^d$ . By learning the parameters of  $d$ , the scores can reflect the rank of the frames, i.e.  $S(q|d) > S(t|d)$  when  $q > t$ . In the last, learning the  $d$  can be considered as a convex optimization problem which can be solved by the RankSVM formulation:

$$d^* = \rho(R_1, R_2, \dots, R_T; \psi) = \underset{d}{\operatorname{argmin}} E(d),$$

$$E(d) = \frac{\lambda}{2} \|d\|^2 + \frac{2}{T(T-1)} \times \sum \max\{0, 1 - S(q|d) + S(t|d)\}, \quad (1)$$

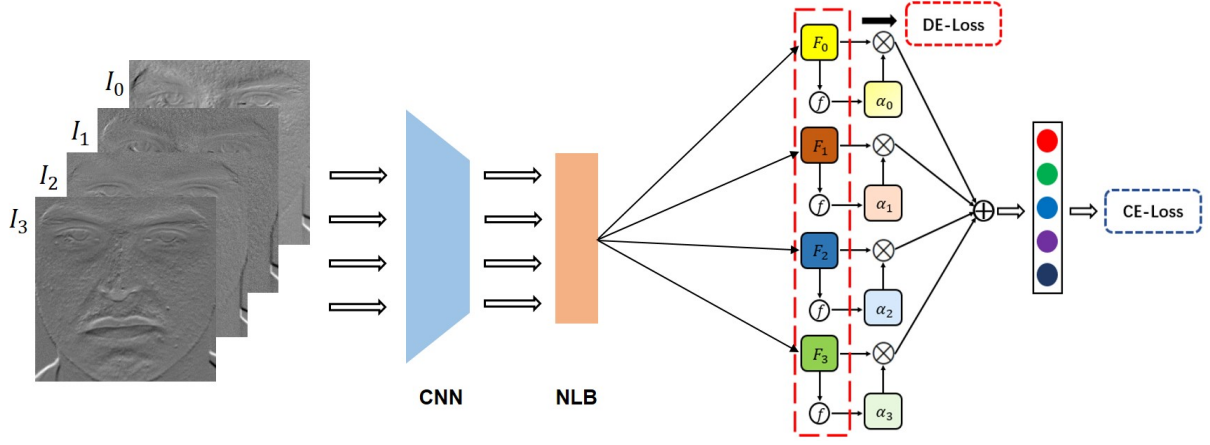


Figure 3: The pipeline of the proposed SMA-STN. Four dynamic images ( $I_0, I_1, I_2, I_3$ ) calculated from a micro-expression sequence by DSSI are input into a CNN backbone for feature extraction. Subsequently, the non-local block (NLB) calculates weights to capture long-range dependencies for facial regions and further processes the features. And then, the global self-attention module learns weights for each dynamic image to obtain DE-Loss. A compact representation is obtained after aggregating all the features with calculated attention ( $\alpha_0, \alpha_1, \alpha_2, \alpha_3$ ) for final classification.

Since it is computational to obtain a dynamic image, an practical approximation to rank pooling called approximate rank pooling (ARP) has been proposed (Bilen et al. 2017)(Bilen et al. 2016). The ARP is derived by considering the first step of Eq. 1 in a gradient-based optimization starting with  $\mathbf{d}^* = \vec{0}$ , and we can obtain the first approximated solution as:  $\mathbf{d}^* = \vec{0} - \eta \nabla E(\mathbf{d})|_{\mathbf{d}=\vec{0}} \propto -\nabla E(\mathbf{d})|_{\mathbf{d}=\vec{0}}$  for any  $\eta > 0$ , where

$$\begin{aligned} \nabla E(\vec{0}) &\propto \sum_{q>t} \nabla \max\{0, 1 - S(q | \mathbf{d}) + S(t | \mathbf{d})\} \Big|_{\mathbf{d}=\vec{0}} \\ &= \sum_{q>t} \nabla \langle \mathbf{d}, V_t - V_q \rangle = \sum_{q>t} V_t - V_q, \end{aligned} \quad (2)$$

then  $d^*$  can be expanded as follows:

$$\mathbf{d}^* \propto \sum_{q>t} V_q - V_t = \sum_{t=1}^T \beta_t V_t, \quad (3)$$

Through expanding above formulation, the coefficients  $\beta_t$  can be writing as scalar:

$$\beta_t = 2t - T - 1, \quad (4)$$

As shown in (Bilen et al. 2017)(Bilen et al. 2016), the feature vector  $\psi(R_t)$  can be replaced by individual video frames  $R_t$ . Thus, the dynamic image computation reduces to accumulating the time average of video frames after pre-multiplying them by  $\beta_t$ . The obtained  $d^*$  has cumulative information which can be used as a spatiotemporal descriptor of a video sequence. Specially, four dynamic images  $\{I_0, I_1, I_2, I_3\}$  related to different segments are calculated from four sampled snippets. From Figure 5, we can find that although it is hard to distinguish different micro-expression images in a continuous sequence since the subtle movement changes, the calculated four dynamic images are significantly different from

each other. That is to say, the subtle movement changes have been magnified successfully by the DSSI module visually.

### Spatiotemporal Movement-Attending Module

A spatiotemporal movement-attending module (STMA) set up with a spatial non-local self-attention block and a global self-attention module is proposed to capture long-distance spatial relation of facial regions and weight different segments of a micro-expression sequence at the same time.

**Spatial Non-local Self-Attention Block.** It is difficult to judge the type of expression based on only a portion of facial regions according to the facial action units (AU) theory (Ekman 1997). Thus, it is significant to capture the long-distance relation to consider the comprehensive information of facial micro-expression to judge its emotion type objectively. To handle this problem, motivated by the 2D gaussian non-local networks (Wang et al. 2018), we utilize the embedded gaussian non-local self-attention block added after the CNN backbone to capture the long-distance dependencies in extracted features. It is obvious that the long-distance relation of micro-expression samples with same emotion category in a sequence are extremely similar to each other, hence the added non-local block shared weights with all the inputs, which is shown in Figure 4. The non-local self-attention block is defined as follows:

$$f_i = W_y \frac{e^{\xi(X_i)^T \psi(X_j)}}{\sum_j e^{\xi(X_i)^T \psi(X_j)}} W_g X_j + X, \quad (5)$$

$$F_i = \rho(f_i), \quad (6)$$

where  $\psi$  and  $\xi$  are convolution operations with stride  $1 \times 1$ ,  $\rho$  denotes the average pooling operation,  $W_y$  and  $W_g$  are the weighting matrixes, and the input  $X$  is the feature map of a dynamic image extracted by the CNN. The core idea of the non-local self-attention block is that more information can be maintained by constructing a convolution operation

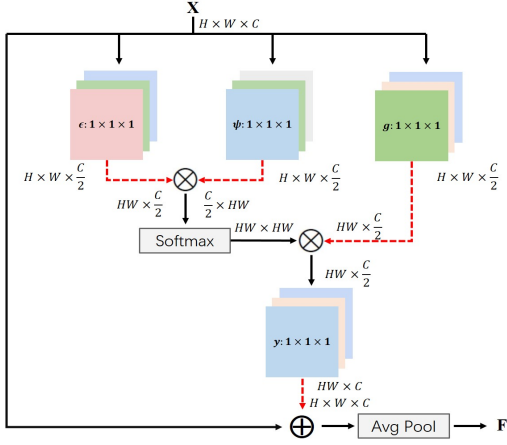


Figure 4: The illustration of the non-local block.  $\otimes$  and  $\oplus$  denote matrix multiplication and elements-wise addition, respectively, and red dashed line denotes matrix reshaping.

whose size is the same as the feature map (Wang et al. 2018).

**Global Self-Attention Module.** It is believed that learning weights from both the local segments and global sequence is more beneficial to classification (Meng et al. 2019). Thus, inspired by the frame-attention network (Meng et al. 2019), a segment-based global self-attention module is embedded after the spatial embedded gaussian non-local self-attention block. To be specific, the weights of dynamic image related to the  $i$ -th segment can be calculated as:

$$\alpha_i = s(\sigma(F_i^T * q)), \quad (7)$$

where  $q$  denotes the parameters of a fully-connected layer,  $\sigma$  denotes the sigmoid function, and  $s$  denotes the softmax function. All the input features are aggregated into a global feature representation with the attention weights as follows:

$$F_m = \sum_{i=0}^n \alpha_i F_i, \quad (8)$$

$F_m$  is used as the representation for the final classification. Through the spatiotemporal movement-attending mechanism, not only the long-distance spatial relation of facial regions but the temporal movement changes can be considered together.

### Deviation Enhancement Regularization

To distinguish dynamic images related to different segments in feature level, we propose a simple yet effective deviation enhancement loss function (DE-Loss) which magnifies the subtle movement changes among dynamic images by enhancing the standard deviation. We firstly measure differences between the four features extracted by the non-local self-attention block through calculating and normalizing the Euclidean distance among them:

$$D_{ij} = \|F_i - F_j\|_2, \quad (9)$$

$$\overline{D_{i,j}} = \frac{D_{i,j} - D_{\min}}{D_{\max} - D_{\min}}, \quad (10)$$

where  $F_i$  and  $F_j$  are the features of dynamic images extracted by the non-local self-attention block ( $i < j$ ).  $D_{\max}$ ,  $D_{\min}$  and  $D_{\text{mean}}$  denote the maximum value, the mean value and the minimum value of  $D_{i,j}$ , respectively. The DE-loss is formulated by adding a margin to the standard deviation of  $D_{i,j}$ :

$$\mathcal{L}_{DE} = 1 - D_{std}, \quad (11)$$

In the training phase, the DE-Loss is jointly trained with the cross-entropy loss. Mathematically, the whole training loss can be formulated as follows:

$$\mathcal{L} = \mathcal{L}_{CE} + \lambda \mathcal{L}_{DE}, \quad (12)$$

where  $\lambda$  is the trade-off parameter.

## Experiments

In this section, we conduct extensive experiments on three public micro-expression databases to validate the performance of the proposed SMA-STN. Especially, we first introduce the used micro-expression databases and implementation details and then compare it to other state-of-the-art MER methods to show the effectiveness of the proposed SMA-STN.

### Databases and Implementation Details

**CASME II** The CASME II database (Yan et al. 2014) is built by Yan et al. from the Institute of Psychology, Chinese Academy of Sciences, which recorded 247 micro-expression examples with action units (AUs) labeled from 27 subjects. These micro-expression examples are collected in a high temporal resolution of 100 fps categorised into five emotion classes, i.e., *Happiness* (32 samples), *Surprise* (25 samples), *Disgust* (64 samples), *Repression* (27 samples), and *Others* (99 samples).

**SAMM** The SAMM database (Davison et al. 2016) is collected by Davison et al. from Manchester City University, which contains 159 micro-expression samples recorded from 29 subjects, and 8 micro-expression classes collected at 200 fps. Note that since the number of some micro-expression classes in the SAMM databases is too small, we only use the micro-expression classes whose number is larger than 10 in the experiment, namely *Anger* (57 samples), *Contempt* (12 samples), *Happiness* (26 samples), *Surprise* (15 samples), and *Others* (26 samples).

**SMIC** The SMIC database (Li et al. 2013) is set up by Li et al. from the University of Oulu, Finland. It consists of 164 samples recorded from 16 subjects in 3 classes of emotions, namely *Positive* (51 samples), *Negative* (70 samples), *Surprise* (43 samples), respectively. Different from the CASME II database, the samples of SMIC database are divided to three parts according to the recording equipment, including a high-speed camera (HS) of 100 fps, a normal visual camera (VIS) of 25 fps, and a near-infrared camera (NIR) of 25 fps. The SMIC-HS database consists of 164 micro-expression clips recorded from 16 subjects, while the SMIC-VIS and SMIC-VIR both have 71 micro-expression samples from 8

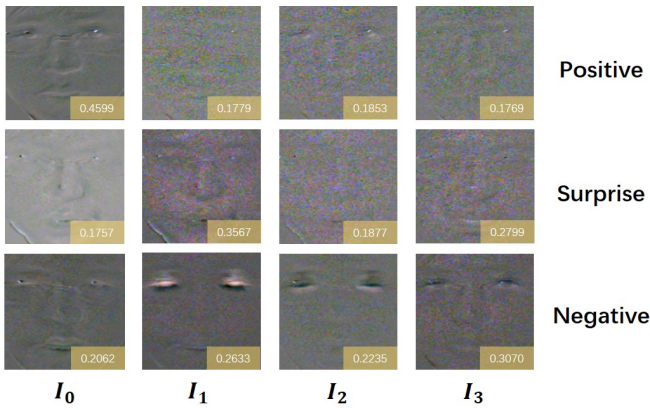


Figure 5: Visualization of the learned  $\alpha$  in SMA-STN. Each row stands for a set of dynamic images computed by DSSI from a micro-expression sequence.

subjects. In this paper, we use the micro-expression samples recorded by a high-speed camera, namely the samples in SMIC-HS database.

**Implementation Details.** In the experiments, the Face++ detection API is used to do the face detection and alignment, and then all the cropped micro-expression samples are resized to  $224 \times 224$ . The proposed SMA-STN is implemented with Pytorch toolbox, and we utilized the ResNet18 (He et al. 2016) pre-trained on Face Attention Network (Wang, Yuan, and Yu 2017) as the CNN backbone. To avoid over fitting, the samples used for training are expanded with clockwise and counterclockwise rotation with  $\pm 5$  and  $\pm 10$  degree and horizontal flip. In the training phase, the initial learning rate is set to  $3 \times 10^{-4}$ , and the training will be stopped in 100 epochs. The SMA-STN is trained in an end-to-end manner with Nvidia Titan Xp GPU. All the experiments are conducted under the leave-one-subject-out (LOSO) protocol since it can avoid samples from the same subject appearing in the training set and validation set, which can make the experimental results more reliable. Thus, only micro-expression data samples of a subject of the database are used for validating, and the remaining micro-expression data samples are used for training.

Table 1: The recognition accuracy and F1-score of different methods under the LOSO protocol on CASME II database.

Methods	Accuracy	F1-score
LBP-TOP(Ngo et al. 2016)	51.00	0.4700
EVM(Li et al. 2017)	67.21	N/A
STCLQP(Huang and Zhao 2017)	58.39	0.5836
FDM(Xu, Zhang, and Wang 2017)	41.96	0.4700
SSSN(Khor et al. 2019)	71.19	0.7151
DSSN(Khor et al. 2019)	70.78	0.7297
TSCNN-I(Song et al. 2019)	74.05	0.7327
TSCNN-II(Song et al. 2019)	80.97	0.8070
<b>SMA-STN(Ours)</b>	<b>82.59</b>	<b>0.7946</b>

\* N/A - no results reported.

## Evaluation of the SMA-STN

**Comparison to the State-of-the-Art.** The experimental results of 3 databases under the LOSO protocol are shown in Table 1, Table 2 and Table 3, respectively. Following the work in (Zong et al. 2018) (Song et al. 2019), two evaluation methods including recognition accuracy and mean F1-score are adopted as the performance metric. To be specific, the F1-score is computed according to  $F1 - score = \frac{1}{c} \sum_{i=1}^c \frac{2p_i \times r_i}{p_i + r_i}$ , where  $p_i$  and  $r_i$  stand for the precision and recall of the  $i$ th micro-expression, and  $c$  denotes the number of micro-expression categories.

Besides, several state-of-the-art methods are used for com-

Table 2: The recognition accuracy and F1-score of different methods under the LOSO protocol on SAMM database.

Methods	Accuracy	F1-score
LBP-TOP(Zhao and Pietikainen 2007)	34.56	0.2892
LBP-SIP(Wang et al. 2015)	36.03	0.3133
HOG-TOP(Li et al. 2017)	36.03	0.3403
HIGO-TOP(Li et al. 2017)	41.18	0.3920
SSSN(Khor et al. 2019)	56.62	0.4513
DSSN(Khor et al. 2019)	57.35	0.4644
TSCNN-I(Song et al. 2019)	63.53	0.6065
TSCNN-II(Song et al. 2019)	71.76	0.6942
<b>SMA-STN(Ours)</b>	<b>77.20</b>	<b>0.7033</b>

parison, including LBP-TOP (Ngo et al. 2016; Zhao and Pietikainen 2007; Liong et al. 2014), LBP-SIP (Wang et al. 2015), EVM + HIGO (Li et al. 2017), STCLQP (Huang and Zhao 2017), HIGO-TOP (Li et al. 2017), LPQ-TOP (Päiväranta, Rahtu, and Heikkilä 2011), FMBH(Lu, Kidiyo, and Joseph 2018), FDM (Xu, Zhang, and Wang 2017), SSSN, DSSN (Khor et al. 2019) and TSCNN (Song et al. 2019). According to the results, we can find that the proposed SMA-STN achieves the best results in both recognition accuracy and F1-score in most cases. Specially, the proposed SMA-STN gets a better performance increase of 1.62% recognition accuracy compared to the state-of-the-art TSCNN-II method on CASME II database, and it achieves promising performance compared to the classic LBP-TOP with an increase of 31.59%/0.3246 in recognition accuracy/F1-score. As for SAMM database, the proposed SMA-STN obtains the best performance according to both recognition accuracy (77.20%) and F1-score (0.7033). Furthermore, the proposed SMA-STN achieves the best results in both recognition accuracy (77.44%) and F1-score (0.7683), which are higher than the state-of-the-art TSCNN-I method by a margin of 4.70% and 0.0447 in recognition accuracy and F1-score on SMIC-HS database.

**Visualization of  $\alpha$  in SMA-STN.** We visualize the learned importance  $\alpha$  during training phase to investigate the effectiveness of SMA-STN to subtle movement changes. As shown in Figure 5, we can find that the calculated dynamic images in a sequence are obviously different from each other, which indicates that the subtle movement changes in a micro-expression sequence are magnified. Furthermore, SMA-STN efficiently enhances the weights of dynamic im-

ages which contains more movement information and suppresses the less ones.

Table 3: The recognition accuracy and F1-score of different methods under the LOSO protocol on SMIC database.

Methods	Accuracy	F1-score
LBP-TOP + TIM(Liong et al. 2014)	33.56	N\A
STCLQP(Huang and Zhao 2017)	64.02	0.6381
FDM(Xu, Zhang, and Wang 2017)	54.88	0.5380
FMBH(Lu, Kidiyo, and Joseph 2018)	71.95	N\A
SSSN(Khor et al. 2019)	63.41	0.6329
DSSN(Khor et al. 2019)	63.41	0.6462
OFF-ApexNet(Gan et al. 2019)	67.68	0.6709
TSCNN-I(Song et al. 2019)	72.74	0.7236
<b>SMA-STN(Ours)</b>	<b>77.44</b>	<b>0.7683</b>

\* N\A - no results reported.

Table 4: Evaluation of the proposed attention and loss function modules in SMA-STN.

Exp	STMA	EA-Loss	Accuracy	F1-score
1	×	×	68.90%	0.6593
2	×	✓	72.56%	0.7218
3	✓	×	74.39%	0.7362
4	✓	✓	<b>77.44%</b>	<b>0.7683</b>

## Ablation Study

An ablation study is conducted on the SMIC-HS database to investigate the generality of the proposed SMA-STN.

**Evaluation of the proposed modules in SMA-STN.** Several experiments are designed on the SMIC-HS database to evaluate the STMA and the DE-Loss in SMA-STN. The experimental results are presented in Table 4. According to the experimental results on recognition accuracy and F1-score, we can draw the following conclusions. First, all of the two modules improve the experimental results compared to the baseline (Exp.1) in varying degrees, which proves their effectiveness in improving MER issue performance. In addition, by adding three modules in turn, we achieve an improvement of 3.66%/0.0625, 5.49%/0.0769 and 8.54%/0.109 in recognition and F1-score in Exp 2, 3 and 4 relative to the baseline experiments, which indicates that the combination of different modules can better improve the experimental results.

**Evaluation of the tradeoff parameter  $\lambda$ .** Several experiments are conducted to evaluate the effect of the difference value of  $\lambda$  reported in Figure 6. It shows that the most proper value of  $\lambda$  to obtain a best result on SMIC-HS is 0.03, which obtains 77.44% and 0.7683 in recognition accuracy and F1-score. Since  $\lambda$  is a tradeoff coefficient to balance the classification cross-entropy and motion intensity magnification loss, the smaller values can not adequately distinguish subtle movement changes in different segments of a micro-expression sequence which results in lower experimental results. In contrast, a massive  $\lambda$  value will make the network

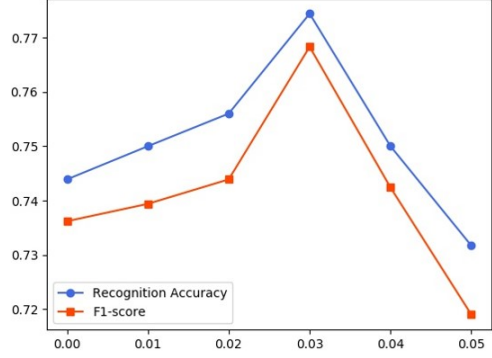


Figure 6: Evaluation of the tradeoff parameter  $\lambda$  on the SMIC-HS database.

ignore the role of cross-entropy and lead to the degradation of classification performance.

## Conclusion

In this paper, we propose an SMA-STN set up with a spatiotemporal movement-attending module (STMA) and a deviation enhancement loss (DE-Loss) to handle the crucial issue of revealing the subtle movement changes while enhancing the significant segments for MER in an efficient way. Besides, a novel dynamic segmented sampling imaging module (DSSI) is also proposed to compute dynamic images from micro-expressions sampled under a unique protocol, which can be considered as a spatiotemporal descriptor to capture the subtle movements while reducing the redundant data simultaneously. The STMA includes a spatial embedded gaussian non-local self-attention block and a global self-attention module to learn the long-distance spatial relation of facial regions and compute attention for divided segments and the whole sequence. The DE-Loss adds the standard deviation regularization in terms of Euclidean distance among extracted features to the SMA-STN, further improving the network's robustness to subtle movement changes in feature level. Through extensive experiments on three widely used micro-expression databases, the proposed SMA-STN outperforms other state-of-the-art methods, which proves its effectiveness on the MER issue.

## References

- Bilen, H.; Fernando, B.; Gavves, E.; and Vedaldi, A. 2017. Action recognition with dynamic image networks. *IEEE transactions on pattern analysis and machine intelligence* 40(12): 2799–2813.
- Bilen, H.; Fernando, B.; Gavves, E.; Vedaldi, A.; and Gould, S. 2016. Dynamic image networks for action recognition. In *Proceedings of the IEEE Conference on Computer Vision and Pattern Recognition*, 3034–3042.
- Davison, A. K.; Lansley, C.; Costen, N.; Tan, K.; and Yap,

- M. H. 2016. Samm: A spontaneous micro-facial movement dataset. *IEEE Transactions on Affective Computing* 9(1): 116–129.
- Ekman, P.; and Friesen, W. V. 1969. Nonverbal leakage and clues to deception. *Psychiatry* 32(1): 88–106.
- Ekman, R. 1997. *What the face reveals: Basic and applied studies of spontaneous expression using the Facial Action Coding System (FACS)*. Oxford University Press, USA.
- Frank, M.; Herbasz, M.; Sinuk, K.; Keller, A.; and Nolan, C. 2009. I see how you feel: Training laypeople and professionals to recognize fleeting emotions. In *The Annual Meeting of the International Communication Association. Sheraton New York, New York City*.
- Frank, M. G.; Maccario, C. J.; and Govindaraju, V. 2009. Behavior and security. Protecting Airline Passengers in the Age of Terrorism.
- Gan, Y. S.; Liong, S.; Yau, W.; Huang, Y.; and Ken, T. L. 2019. OFF-ApexNet on micro-expression recognition system. *Signal Process. Image Commun.* 74: 129–139. doi: 10.1016/j.image.2019.02.005. URL <https://doi.org/10.1016/j.image.2019.02.005>.
- Haggard, E. A.; and Isaacs, K. S. 1966. Micromomentary facial expressions as indicators of ego mechanisms in psychotherapy. In *Methods of research in psychotherapy*, 154–165. Springer.
- He, K.; Zhang, X.; Ren, S.; and Sun, J. 2016. Deep residual learning for image recognition. In *Proceedings of the IEEE conference on computer vision and pattern recognition*, 770–778.
- Huang, X.; and Zhao, G. 2017. Spontaneous facial micro-expression analysis using spatiotemporal local radon-based binary pattern. In *2017 International Conference on the Frontiers and Advances in Data Science (FADS)*.
- Khor, H.; See, J.; Liong, S.; Phan, R. C.; and Lin, W. 2019. Dual-stream Shallow Networks for Facial Micro-expression Recognition. In *2019 IEEE International Conference on Image Processing, ICIP 2019, Taipei, Taiwan, September 22–25, 2019*, 36–40. IEEE. doi:10.1109/ICIP.2019.8802965. URL <https://doi.org/10.1109/ICIP.2019.8802965>.
- Li, X.; Hong, X.; Moilanen, A.; Huang, X.; Pfister, T.; Zhao, G.; and Pietikainen, M. 2017. Towards Reading Hidden Emotions: A Comparative Study of Spontaneous Micro-expression Spotting and Recognition Methods. *IEEE Transactions on Affective Computing* 1–1.
- Li, X.; Pfister, T.; Huang, X.; Zhao, G.; and Pietikainen, M. 2013. A spontaneous micro-expression database: Inducement, collection and baseline. In *2013 10th IEEE International Conference and Workshops on Automatic Face and Gesture Recognition (FG)*, 1–6. IEEE.
- Liong, S.; Phan, R. C.; See, J.; Oh, Y.; and Wong, K. 2014. Optical strain based recognition of subtle emotions. In *International Symposium on Intelligent Signal Processing and Communication Systems, ISPACS 2014, Kuching, Sarawak, Malaysia, December 1–4, 2014*, 180–184. IEEE. doi:10.1109/ISPACS.2014.7024448. URL <https://doi.org/10.1109/ISPACS.2014.7024448>.
- Liu, Y.-J.; Li, B.-J.; and Lai, Y.-K. 2018. Sparse MDMO: Learning a discriminative feature for spontaneous micro-expression recognition. *IEEE Transactions on Affective Computing*.
- Lu, H.; Kidiyo, K.; and Joseph, R. 2018. Motion descriptors for micro-expression recognition. *Signal Processing Image Communication* S0923596518303540–.
- Meng, D.; Peng, X.; Wang, K.; and Qiao, Y. 2019. frame attention networks for facial expression recognition in videos. In *2019 IEEE International Conference on Image Processing (ICIP)*, 3866–3870. IEEE.
- Ngo, A. C. L.; Oh, Y.; Phan, R. C.; and See, J. 2016. Eulerian emotion magnification for subtle expression recognition. In *2016 IEEE International Conference on Acoustics, Speech and Signal Processing, ICASSP 2016, Shanghai, China, March 20–25, 2016*, 1243–1247. IEEE. doi: 10.1109/ICASSP.2016.7471875. URL <https://doi.org/10.1109/ICASSP.2016.7471875>.
- O’Sullivan, M.; Frank, M. G.; Hurley, C. M.; and Tiwana, J. 2009. Police lie detection accuracy: The effect of lie scenario. *Law and Human Behavior* 33(6): 530.
- Pfister, T.; Li, X.; Zhao, G.; and Pietikainen, M. 2011. Recognising spontaneous facial micro-expressions. In *2011 international conference on computer vision*, 1449–1456. IEEE.
- Polikovskiy, S.; Kameda, Y.; and Ohta, Y. 2009. Facial micro-expressions recognition using high speed camera and 3D-gradient descriptor.
- Päivärinta, J.; Rahtu, E.; and Heikkilä, J. 2011. Volume Local Phase Quantization for Blur-Insensitive Dynamic Texture Classification. In *Image Analysis-scandinavian Conference*.
- Song, B.; Li, K.; Zong, Y.; Zhu, J.; Zheng, W.; Shi, J.; and Zhao, L. 2019. Recognizing Spontaneous Micro-Expression Using a Three-Stream Convolutional Neural Network. *IEEE Access* 7: 184537–184551.
- Vaswani, A.; Shazeer, N.; Parmar, N.; Uszkoreit, J.; Jones, L.; Gomez, A. N.; Kaiser, Ł.; and Polosukhin, I. 2017. Attention is all you need. In *Advances in neural information processing systems*, 5998–6008.
- Verma, M.; Vipparthi, S. K.; Singh, G.; and Murala, S. 2019. LEARNet: Dynamic Imaging Network for Micro Expression Recognition. *IEEE Transactions on Image Processing* 29: 1618–1627.
- Wang, J.; Yuan, Y.; and Yu, G. 2017. Face attention network: An effective face detector for the occluded faces. *arXiv preprint arXiv:1711.07246*.
- Wang, K.; Peng, X.; Yang, J.; Meng, D.; and Qiao, Y. 2019. Region attention networks for pose and occlusion robust facial expression recognition. *arXiv preprint arXiv:1905.04075*.

Wang, L.; Xiong, Y.; Wang, Z.; Qiao, Y.; Lin, D.; Tang, X.; and Van Gool, L. 2016. Temporal segment networks: Towards good practices for deep action recognition. In *European conference on computer vision*, 20–36. Springer.

Wang, S.-J.; Yan, W.-J.; Zhao, G.; Fu, X.; and Zhou, C.-G. 2014. Micro-expression recognition using robust principal component analysis and local spatiotemporal directional features. In *European Conference on Computer Vision*, 325–338. Springer.

Wang, X.; Girshick, R.; Gupta, A.; and He, K. 2018. Non-local neural networks. In *Proceedings of the IEEE conference on computer vision and pattern recognition*, 7794–7803.

Wang, Y.; See, J.; Phan, W.; and Oh, Y. H. 2015. LBP with Six Intersection Points: Reducing Redundant Information in LBP-TOP for Micro-expression Recognition. In *Accv*.

Xia, Z.; Hong, X.; Gao, X.; Feng, X.; and Zhao, G. 2019. Spatiotemporal recurrent convolutional networks for recognizing spontaneous micro-expressions. *IEEE Transactions on Multimedia*.

Xu, F.; Zhang, J.; and Wang, J. Z. 2017. Microexpression Identification and Categorization Using a Facial Dynamics Map. *IEEE Trans. Affect. Comput.* 8(2): 254–267. doi:10.1109/TAFFC.2016.2518162. URL <https://doi.org/10.1109/TAFFC.2016.2518162>.

Yan, W.-J.; Li, X.; Wang, S.-J.; Zhao, G.; Liu, Y.-J.; Chen, Y.-H.; and Fu, X. 2014. CASME II: An improved spontaneous micro-expression database and the baseline evaluation. *PloS one* 9(1).

Yang, J.; Ren, P.; Zhang, D.; Chen, D.; Wen, F.; Li, H.; and Hua, G. 2017. Neural aggregation network for video face recognition. In *Proceedings of the IEEE conference on computer vision and pattern recognition*, 4362–4371.

Zhao, G.; and Pietikainen, M. 2007. Dynamic Texture Recognition Using Local Binary Patterns with an Application to Facial Expressions. *IEEE Transactions on Pattern Analysis and Machine Intelligence* 29: p.915–928.

Zong, Y.; Huang, X.; Zheng, W.; Cui, Z.; and Zhao, G. 2018. Learning from hierarchical spatiotemporal descriptors for micro-expression recognition. *IEEE Transactions on Multimedia* 20(11): 3160–3172.